

# Efficacy of a Third-Generation Oncolytic Herpes Virus G47 $\Delta$ in Advanced Stage Models of Human Gastric Cancer

Kotaro Sugawara,<sup>1,2</sup> Miwako Iwai,<sup>1</sup> Shoh Yajima,<sup>1,2</sup> Minoru Tanaka,<sup>1</sup> Kazuyoshi Yanagihara,<sup>3</sup> Yasuyuki Seto,<sup>2</sup> and Tomoki Todo<sup>1</sup>

<sup>1</sup>Division of Innovative Cancer Therapy, Advanced Clinical Research Center, Institute of Medical Science, The University of Tokyo, Tokyo 108-8639, Japan; <sup>2</sup>Department of Gastrointestinal Surgery, Graduate School of Medicine, The University of Tokyo, Tokyo 113-8655, Japan; <sup>3</sup>Division of Biomarker Discovery, Exploratory Oncology Research and Clinical Trial Center, National Cancer Center, Chiba 277-8577, Japan

**Advanced gastric cancer, especially scirrhous gastric cancer with peritoneal dissemination, remains refractory to conventional therapies. G47 $\Delta$ , a third-generation oncolytic herpes simplex virus type 1, is an attractive novel therapeutic agent for solid cancer. In this study, we investigated the therapeutic potential of G47 $\Delta$  for human gastric cancer. *In vitro*, G47 $\Delta$  showed good cytopathic effects and replication capabilities in nine human gastric cancer cell lines tested. *In vivo*, intratumoral inoculations with G47 $\Delta$  ( $2 \times 10^5$  or  $1 \times 10^6$  plaque-forming units [PFU]) significantly inhibited the growth of subcutaneous tumors (MKN45, MKN74, and 44As3). To evaluate the efficacy of G47 $\Delta$  for advanced-stage models of gastric cancer, we generated an orthotopic tumor model and peritoneal dissemination models of human scirrhous gastric cancer (MKN45-luc and 44As3Luc), which have features mimicking intractable scirrhous cancer patients. G47 $\Delta$  ( $1 \times 10^6$  PFU) was constantly efficacious whether administered intratumorally or intraperitoneally in the clinically relevant models. Notably, G47 $\Delta$  injected intraperitoneally readily distributed to, and selectively replicated in, disseminated tumors. Furthermore, flow cytometric analyses of tumor-infiltrating cells in subcutaneous tumors revealed that intratumoral G47 $\Delta$  injections markedly decreased M2 macrophages while increasing M1 macrophages and natural killer (NK) cells. These findings indicate the usefulness of G47 $\Delta$  for treating human gastric cancer, including scirrhous gastric cancer and the ones in advanced stages.**

## INTRODUCTION

Gastric cancer is the third leading cause of cancer mortality worldwide, despite improvements in multimodal treatment strategies.<sup>1</sup> Curative gastrectomy is the principal treatment for gastric cancer, and cytotoxic chemotherapy is generally used when the cancer is unresectable.<sup>2</sup> Although new drugs, such as ramucirumab and nivolumab,<sup>3,4</sup> are available, treatment options are still limited for gastric cancer that progressed after the standard first-line chemotherapy. In particular, the prognosis of patients with peritoneal metastases is

quite poor, which is often the case with scirrhous gastric cancer.<sup>5-7</sup> New treatment strategies for such refractory gastric cancer patients are eagerly awaited.

Oncolytic viruses are genetically engineered or naturally occurring viruses that can selectively replicate in and kill cancer cells without damaging normal tissues.<sup>8</sup> Oncolytic virus therapy has been emerging as a promising new approach to treating cancers, including gastrointestinal tumors.<sup>9</sup> Talimogene laherparepvec (T-VEC), a second-generation oncolytic herpes simplex virus type 1 (HSV-1) expressing granulocyte-macrophage colony-stimulating factor (GM-CSF), was the first to be approved for patients with advanced melanoma in 2015 by the US Food and Drug Administration.<sup>10</sup>

G47 $\Delta$  is a triple-mutated, third-generation oncolytic HSV-1, which was developed by adding another deletion mutation to the genome of a second-generation oncolytic HSV-1, G207.<sup>11,12</sup> In preclinical studies, G47 $\Delta$  exhibited robust antitumor efficacy while retaining excellent safety features.<sup>11,13,14</sup> The first-in-man clinical trial in patients with glioblastoma (UMIN-CTR: UMIN000002661) demonstrated the safety of G47 $\Delta$  inoculated into the human brain. The subsequent investigator-initiated phase II clinical trial (UMIN-CTR: UMIN000015995) in patients with glioblastoma has recently been completed with very good results. Not only for brain tumors, but G47 $\Delta$  should also be applicable to various types of solid cancer. Whereas other oncolytic virus therapies have been investigated in mouse models with subcutaneous tumors or peritoneal dissemination of gastric cancer,<sup>15-19</sup> the efficacy of G47 $\Delta$  for human gastric cancer has never been assessed, and no studies have examined the usefulness

Received 1 March 2020; accepted 26 March 2020;  
<https://doi.org/10.1016/j.omto.2020.03.022>

**Correspondence:** Tomoki Todo, MD, PhD, Division of Innovative Cancer Therapy, Advanced Clinical Research Center, Institute of Medical Science, The University of Tokyo, 4-6-1 Shirokanedai, Minato-ku, Tokyo 108-8639, Japan.  
**E-mail:** [toudou-nsu@umin.ac.jp](mailto:toudou-nsu@umin.ac.jp)



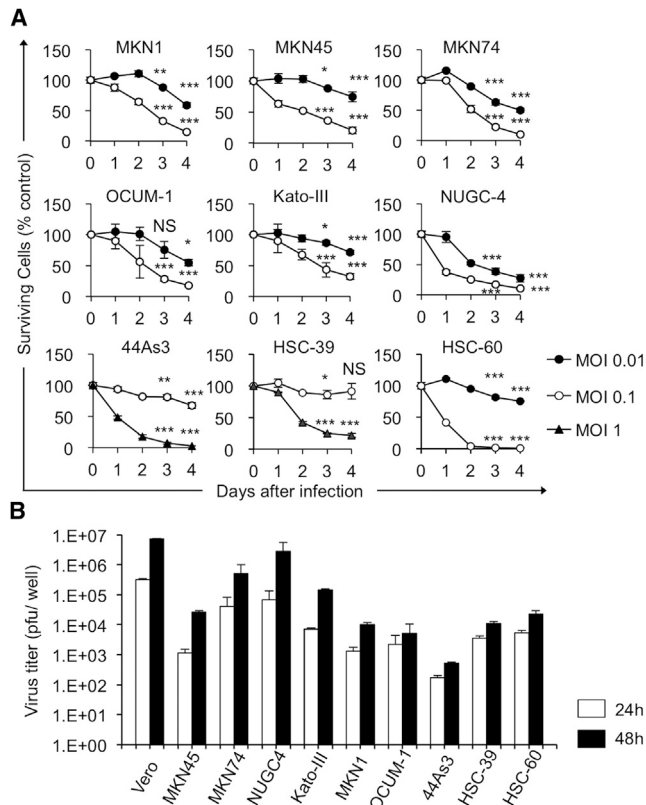


**Figure 1. Cytopathic Effects and Virus Yields of G47 $\Delta$  in Human Gastric Cancer (GC) Cell Lines**

(A) Cells were seeded onto six-well plates at  $2 \times 10^5$  cells/well or onto 96-well plates at optimal cell density. After an overnight incubation, the cells were infected with G47 $\Delta$  (44As3, HSC-39, MOI of 0.1 [O] or 1 [▲]; other cells, MOI of 0.01 [●], 0.1 [O], or mock). The cell viability was determined daily either by counting surviving cells with a Coulter Counter or by the CellTiter 96 Aqueous non-radioactive cell proliferation assay. The percentage of surviving cells is expressed as a percentage of mock-infected controls on each day. G47 $\Delta$  exhibited a good cytopathic effect in the majority of human GC cell lines tested at an MOI of 0.01, whereas some of the cell lines such as 44As3 and HSC-39 were resistant to G47 $\Delta$ , even at an MOI of 0.1. Data are presented as the mean of triplicates  $\pm$  SD. One-way ANOVA followed by a Dunnett's test was used to determine statistical significance (\* $p < 0.05$ , \*\* $p < 0.01$ , \*\*\* $p < 0.001$ , NS, not significant; versus mock-infected controls). (B) Cells were seeded onto six-well plates at  $3 \times 10^5$  cells/well. Triplicate wells were infected with G47 $\Delta$  at an MOI of 0.01. At 24 or 48 h after infection, cells were collected and progeny virus was titered on Vero cells. In most cell lines tested, G47 $\Delta$  showed good replication capability by 48 h after infection, but with exceptions such as 44As3. The results presented are the mean of triplicates  $\pm$  SD.

of oncolytic virus therapy in models of scirrhous gastric cancer or orthotopic gastric cancer.

In this study, we investigate the efficacy of G47 $\Delta$  for human gastric cancer, including scirrhous gastric cancer *in vitro* and *in vivo*. We further examine the usefulness of G47 $\Delta$  for advanced-stage gastric cancer using an orthotopic tumor model and peritoneal dissemination models. In addition, immune responses accompanying G47 $\Delta$  treatment are investigated by analyzing tumor-infiltrating immune cells.

## RESULTS

### Cytopathic Effect and Replication Capability of G47 $\Delta$ *In Vitro*

To characterize the oncolytic activity of G47 $\Delta$  in gastric cancer, we studied its cytopathic effects and replication capabilities in nine human gastric cancer cell lines *in vitro*. In the cell lines tested, with the exceptions of 44As3 and HSC-39, G47 $\Delta$  at a multiplicity of infection (MOI) of 0.1 showed >70% cell destruction within 4 days after infection (Figure 1A). 44As3 cells and HSC-39 cells, both of which are established from scirrhous gastric cancer, were relatively resistant to killing by G47 $\Delta$  at an MOI of 0.1, although both were effectively killed by G47 $\Delta$  at an MOI of 1 by day 4 (Figure 1A). The yield of progeny virus increased by 48 h after infection at an MOI of 0.01 in most cell lines tested, although the extent of replication varied among cell lines (Figure 1B). These observations indicate that good cytopathic effect and replication capability of G47 $\Delta$  are shown in the majority of human gastric cell lines, whereas some cell lines can be relatively resistant.

### Efficacy of G47 $\Delta$ in Subcutaneous Tumor Models

To study the antitumor efficacy of G47 $\Delta$  *in vivo*, we used three mouse models with subcutaneous tumors of gastric cancer. Athymic mice harboring MNK45, MKN74, and 44As3 tumors of approximately 6 mm in diameter were inoculated intratumorally with G47 $\Delta$  ( $2 \times 10^5$  or  $1 \times 10^6$  plaque-forming units [PFU]) or mock twice (days 0 and 3). In all subcutaneous tumor models, G47 $\Delta$  treatment significantly inhibited tumor growth compared with mock treatment (MKN45,  $p < 0.01$  on day 24; MKN74,  $p < 0.01$  on day 31; 44As3,  $p < 0.01$  on day 15; Figure 2A). Furthermore, in all tumor models, G47 $\Delta$  used at a low dose ( $2 \times 10^5$  PFU) was as effective as G47 $\Delta$  at a high dose ( $1 \times 10^6$  PFU). We further investigated the efficacy of G47 $\Delta$  treatment for large subcutaneous tumors. G47 $\Delta$  treatment significantly inhibited tumor growth compared with mock treatment even for large subcutaneous tumors ( $\geq 200$  mm<sup>3</sup>) (MKN45,  $p < 0.01$  on day 19; 44As3,  $p < 0.01$  on day 31; Figure 2B).

### Intratumoral G47 $\Delta$ Treatment Inhibited the Growth of Orthotopic Tumors

To determine whether G47 $\Delta$  can inhibit the growth of orthotopic tumors, we used an orthotopic tumor model of 44As3Luc. This model has many of the clinical features of scirrhous gastric cancer: Tumor-bearing mice exhibit peritoneal metastases with bloody ascites, resulting in early (within 3–9 weeks) deaths, which mimics the progression to an advanced stage.<sup>20</sup> The experimental design is depicted in Figure 3A. Female athymic mice were inoculated with 44As3Luc ( $1.0 \times 10^6$  cells) into the gastric wall. The mice were divided into two groups on day 7, at which time there was no significant difference in the total photon counts of orthotopic tumors between the two groups (data not shown). On day 8, the establishment of orthotopic tumors was macroscopically confirmed (Figure 3B). Intratumoral inoculations with G47 $\Delta$  ( $1 \times 10^6$  PFU, on days 8 and 11) significantly inhibited the growth of orthotopic tumors ( $p = 0.04$  on day 27, Figure 3C), resulting in improved survival of tumor-bearing mice (median survival time [MST], 68 days versus 55 days;  $p = 0.004$ ; Figure 3D). Two representative cases from each group are shown in Figure 3E.

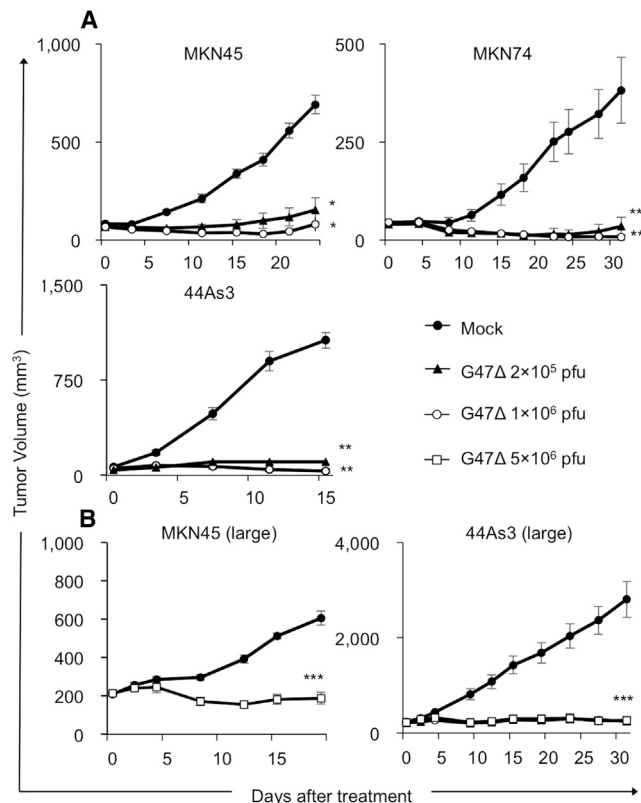


**Figure 2. Antitumor Efficacy of G47 $\Delta$  in GC Subcutaneous Tumor Models**

(A) Subcutaneous tumors from three human GC cell lines (MKN45 [upper left], MKN74 [upper right], and 44As3 [lower left]) were generated in 6-week-old female athymic mice. Established tumors, 5–6 mm in diameter, were inoculated with G47 $\Delta$  ( $2 \times 10^5$  or  $1 \times 10^6$  PFU) or mock on days 0 and 3. G47 $\Delta$  treatment significantly inhibited the tumor growth compared with mock treatment in all GC tumor models irrespective of the dose used. The results presented are the mean  $\pm$  SEM ( $n = 7$ ). (B) Established MKN45 and 44As3 subcutaneous tumors were inoculated with G47 $\Delta$  ( $1 \times 10^6$  PFU) or mock on days 0, 2, and 4 when the tumor volumes exceeded 200 mm<sup>3</sup>. G47 $\Delta$  treatment significantly inhibited the tumor growth compared with mock treatment in both GC tumor models. The results presented are the mean  $\pm$  SEM ( $n = 7$ ). One-way ANOVA followed by a Dunnett's test was used to determine statistical significance (\* $p < 0.05$ , \*\* $p < 0.01$ , \*\*\* $p < 0.001$ ; NS, not significant).

### Efficacy of G47 $\Delta$ in Peritoneal Dissemination Models

To examine whether G47 $\Delta$  is useful for treating gastric cancer in an advanced stage, we studied the efficacy of intraperitoneal G47 $\Delta$  injection using two peritoneal dissemination models of gastric cancer. In order to monitor tumor growth and therapeutic efficacy with an *in vivo* imaging system (IVIS), we used two luciferase-expressing cell lines, MKN45-luc and 44As3Luc. Athymic mice bearing MKN45-luc peritoneal tumors were divided into two groups on day 3, at which time total photon counts did not differ between the two groups (data not shown). Two intraperitoneal injections with G47 $\Delta$  ( $1 \times 10^6$  PFU, on days 4 and 7) significantly inhibited the growth of peritoneal tumors ( $p < 0.01$  on day 24, Figure 4A) and prolonged the survival of tumor-bearing mice (MST, 57 days versus 30 days;  $p <$

0.01; Figure 4B). Two representative cases from each group are shown in Figure 4C. Another peritoneal dissemination model of scirrhous gastric cancer (44As3Luc) similarly showed that two intraperitoneal injections with G47 $\Delta$  ( $1 \times 10^6$  PFU, on days 4 and 7) significantly suppressed the growth of peritoneal tumors ( $p < 0.01$  on day 7, Figure 4D) and prolonged the survival of tumor-bearing mice (MST, 40 days versus 13 days;  $p < 0.01$ ; Figure 4E). Two representative cases from each group are shown in Figure 4F. Furthermore, we studied the efficacy of intraperitoneal injections with G47 $\Delta$  for mice bearing 44As3Luc peritoneal tumors using a virus dose ( $5 \times 10^6$  PFU, on days 3, 5 and 7; Figure 4G) and treatment timing ( $1 \times 10^6$  PFU, on days 1, 3 and 5; Figure 4J) different from the original experiment. In both of these experimental settings, the efficacy of intraperitoneal G47 $\Delta$  treatment was potentiated, especially when the initial treatment started early. (At the high-dose setting, two mice were cured, two died, and six survived at day 50 [Figures 4H and 4I]; at the early timing setting, seven mice were cured, none died, and three survived at day 50 [Figure 4K and 4L]). Results from both models indicate that G47 $\Delta$  exerts strong therapeutic efficacy for peritoneal dissemination of gastric cancer, including scirrhous gastric cancer.

### Distribution of Intraperitoneally Injected G47 $\Delta$

To investigate whether intraperitoneally injected G47 $\Delta$  selectively distributes to metastatic gastric cancer in the peritoneum, T-luc ( $2 \times 10^6$  PFU), a luciferase-expressing oncolytic HSV-1 with the same backbone as G47 $\Delta$ , was intraperitoneally injected into athymic mice bearing peritoneal dissemination of MKN45, and IVIS images were acquired 4 days after treatment. Macroscopically, diffuse peritoneal metastases were recognized in the omentum and mesentery (Figure 5, left). Subsequent IVIS imaging revealed that intraperitoneally injected T-luc was replicating selectively in metastatic tumors of the peritoneum (Figure 5, right).

### Immune Responses Induced by Intratumoral G47 $\Delta$ Treatment

Oncolytic virus therapy reportedly enhances local immune responses, as reflected by the changes in intratumoral macrophages and natural killer (NK) cells, which are crucial for initial priming of antitumor immunity.<sup>21</sup> To study the immune responses in tumors treated by G47 $\Delta$ , athymic mice bearing MKN45 subcutaneous tumors were inoculated intratumorally with G47 $\Delta$  ( $1 \times 10^6$  PFU) or mock. Tumor tissues were harvested 2 days after the treatment, and tumor-infiltrating cells were analyzed by flow cytometry.

G47 $\Delta$  treatment significantly increased the absolute number of intratumoral CD45<sup>+</sup> cells compared with mock treatment ( $p = 0.007$ , Figure 6A). The total number of intratumoral macrophages (CD45<sup>+</sup>CD11b<sup>+</sup>F4/80<sup>+</sup>) did not differ significantly between the two groups ( $p = 0.10$ , Figure 6B), whereas NK cells (CD45<sup>+</sup>CD49b<sup>+</sup>) were significantly increased in the G47 $\Delta$  treatment group ( $p < 0.001$ , Figure 6C). The ratio of M2 macrophages (CD206<sup>+</sup>CD86<sup>-</sup> macrophages) to total macrophages was significantly reduced in the G47 $\Delta$  treatment group ( $p < 0.001$ , Figure 6D), whereas the ratio of M1 macrophages (CD206<sup>-</sup>CD86<sup>+</sup> macrophages) to total macrophages was significantly increased in the G47 $\Delta$  treatment group ( $p = 0.02$ , Figure 6E),

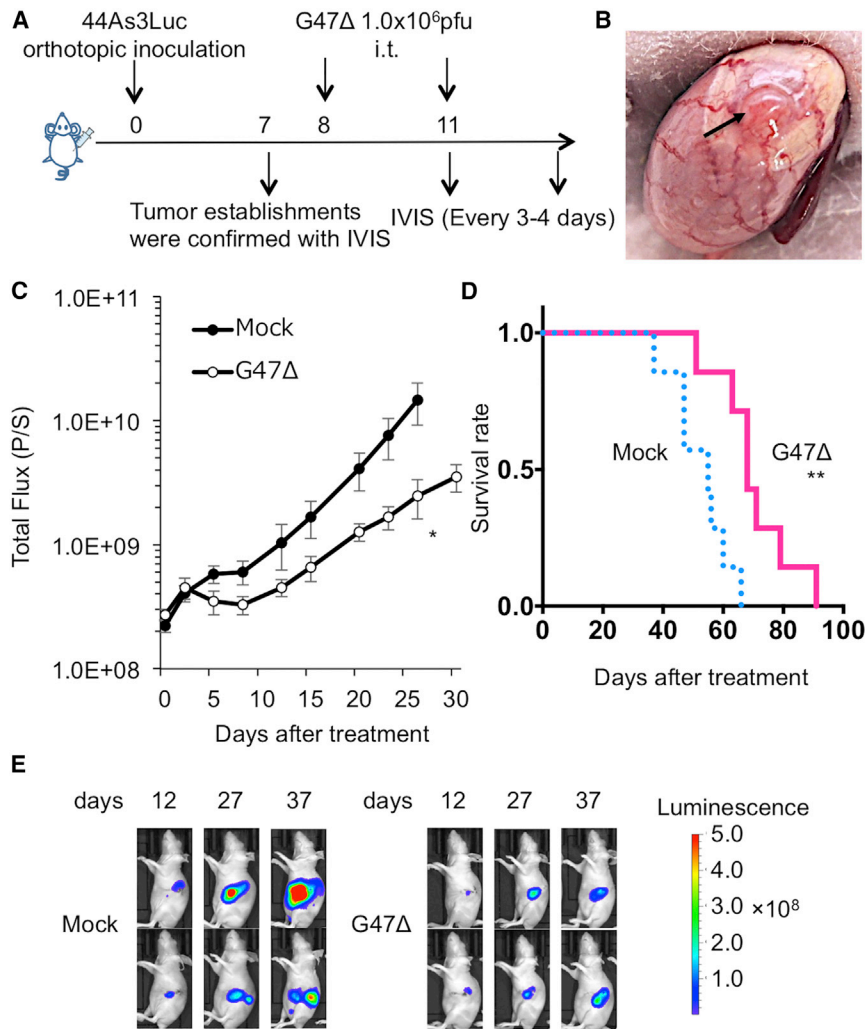


**Figure 3. Efficacy of G47Δ in an Orthotopic Scirrhous Gastric Tumor Model**

(A) Experimental design. Female athymic mice were orthotopically inoculated with 44As3Luc cells ( $1.0 \times 10^6$  cells) into the gastric wall. After confirmation of the orthotopic tumors with IVIS imaging on day 7, the mice were divided into two groups and were treated by intratumoral inoculation with G47Δ ( $1 \times 10^6$  PFU) or mock on days 8 and 11. (B) The established orthotopic gastric tumor was macroscopically confirmed on day 8. (C) The photon counts of the tumors were calculated with IVIS imaging every 3–4 days. G47Δ treatment significantly decreased the total bioluminescence from tumors ( $p = 0.04$  on day 27). (D) G47Δ treatment prolonged the survival of tumor-bearing mice ( $p = 0.004$ ). (E) Two representative cases from each group are shown. The results presented are the mean  $\pm$  SEM ( $n = 7$ ). The Mann-Whitney U test was used to analyze the total bioluminescence from tumors, and the survival was analyzed by the Kaplan-Meier method using the log rank test (\* $p < 0.05$ , \*\* $p < 0.01$ , \*\*\* $p < 0.001$ ; NS, not significant).

present study, G47Δ, a third-generation oncolytic HSV-1, shows a high therapeutic potential for human gastric cancer, even in advanced stages, such that a robust efficacy of G47Δ was observed in an orthotopic tumor model as well as in peritoneal dissemination models.

G47Δ was derived from G207 by creating a further deletion within the nonessential  $\alpha 47$  gene.<sup>11</sup> This added modification conferred enhanced viral replication capability in tumor cells and restored major histocompatibility complex (MHC) class I expression in infected human cells,<sup>13</sup> resulting in enhanced efficacy

resulting in a significant increase in the M1-to-M2 ratio in the G47Δ treatment group ( $p = 0.03$ , Figure 6F).

#### qPCR Analysis of MKN45 Subcutaneous Tumors Treated with G47Δ

Gene expression analysis of MKN45 subcutaneous tumors revealed a significant increase in a gene related to macrophages (*Cd68*) after G47Δ treatment (Figure 7A,  $p < 0.01$ ). Notably, a significant increase in *Cd86*, an M1 macrophage marker, was observed in the G47Δ group (Figure 7B,  $p < 0.001$ ). In contrast, gene expressions of *Arg1* and *Mrc1*, both M2 macrophage markers, were significantly downregulated in G47Δ-treated tumors (Figure 7D,  $p < 0.01$ ; Figure 7E,  $p = 0.04$ , respectively). Overall, these results of qPCR analysis supported the findings from flow cytometric analysis (Figure 6).

#### DISCUSSION

The unsatisfactory treatment outcomes of gastric cancer patients underscore the urgent need for innovative treatment strategies.<sup>2</sup> In the

while retaining the safety features.<sup>11</sup> In the course of clinical development, G47Δ was designated as a “Sakigake” breakthrough therapy drug in Japan, allowing its fact-track drug approval. In addition to clinical trials for glioblastoma, phase I studies have been conducted in patients with prostate cancer (UMIN-CTR: UMIN000010463), olfactory neuroblastoma (UMIN-CTR: UMIN000011636), and malignant pleural mesothelioma (UMIN-CTR: UMIN000034063). The antitumor activity of G47Δ is attributable to several different mechanisms, including selective replication in tumor cells and direct cytotoxicity,<sup>11,13</sup> induction of both innate and adaptive antitumor immune responses, and modification of the tumor microenvironment.<sup>22–25</sup> In addition, G47Δ efficiently kills cancer stem cells,<sup>26</sup> counteracts the angiogenesis induced by oncolytic HSV-1, and can be engineered to express therapeutic genes that further enhance the efficacy.<sup>14,15,27,28</sup>

Good cytopathic effects and replication capabilities of G47Δ were demonstrated in all gastric cancer cell lines tested *in vitro*, including

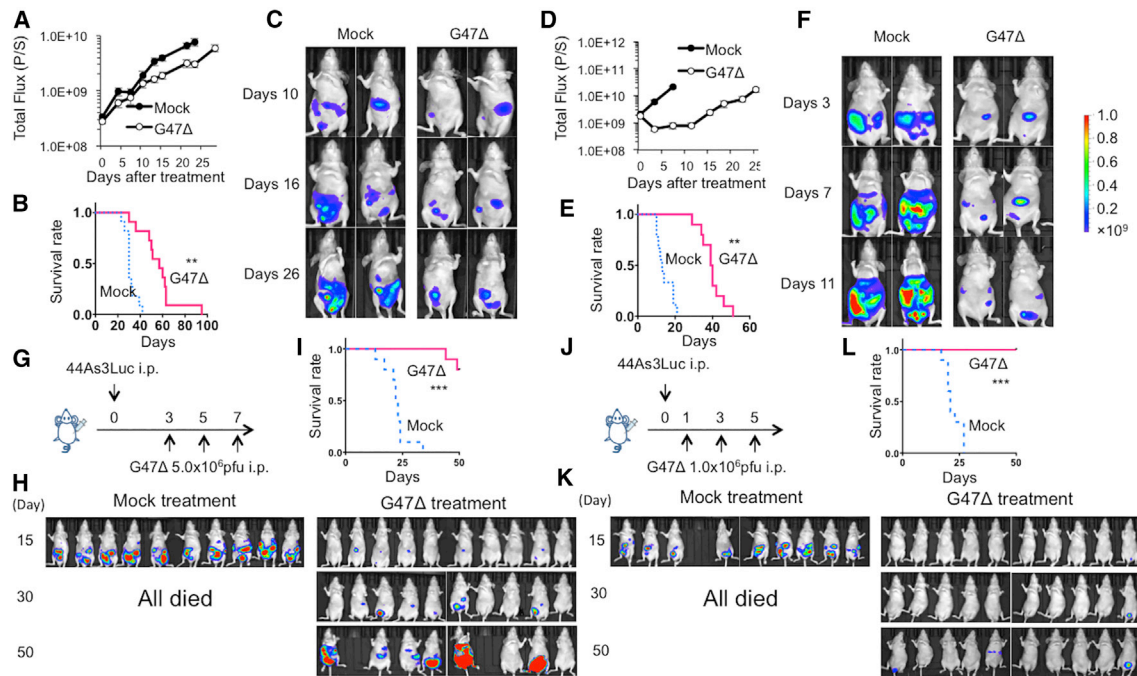


**Figure 4. Efficacy of G47Δ in Peritoneal Dissemination Models**

(A–C) Female athymic mice were intraperitoneally injected with MKN45-luc cells ( $5.0 \times 10^6$  cells). Mice were divided into two groups on day 3 and then intraperitoneally injected with G47Δ ( $1 \times 10^6$  PFU) or mock on days 4 and 7. (A) The photon counts of peritoneal tumors were calculated with IVIS imaging every 3–4 days. G47Δ treatment significantly decreased the total bioluminescence from disseminated tumors ( $p < 0.01$  on day 24). (B) G47Δ treatment prolonged the survival of tumor-bearing mice ( $p < 0.01$ ). (C) Two representative cases from each group are shown. (D–F) A peritoneal dissemination model was generated with 44As3Luc cells ( $1.0 \times 10^6$  cells) in female athymic mice, and the same experiment was performed as above. (D) G47Δ treatment significantly decreased the total bioluminescence from disseminated tumors ( $p < 0.01$  on day 7). (E) G47Δ treatment prolonged the survival ( $p < 0.01$ ) of tumor-bearing mice. (F) Two representative cases from each group are shown. The results presented are the mean  $\pm$  SEM ( $n = 11$  and  $n = 10$ , respectively). A Student's *t* test was used to determine the statistical significance (\*\* $p < 0.01$ ). Survival was analyzed by the Kaplan-Meier method using the log rank test (\*\* $p < 0.01$ ). (G–I) Female athymic mice were intraperitoneally injected with 44As3Luc cells ( $1.0 \times 10^6$  cells). (G) Mice were divided into two groups on day 3 and then intraperitoneally injected with G47Δ ( $5 \times 10^6$  PFU) or mock on days 3, 5, and 7. (H) In the G47Δ treatment group, two mice were cured, two died, and six survived at day 50. All mice died within 30 days in the mock treatment group. (I) G47Δ treatment prolonged the survival of tumor-bearing mice significantly ( $p < 0.001$ ). (J–L) Female athymic mice were intraperitoneally injected with 44As3Luc cells ( $1.0 \times 10^6$  cells). (J) Mice were intraperitoneally injected with G47Δ ( $1 \times 10^6$  PFU) or mock on days 1, 3, and 5. (K) In the G47Δ treatment group, seven mice were cured, none died, and three survived at day 50. All mice died within 30 days in the mock treatment group. (L) G47Δ treatment prolonged the survival of tumor-bearing mice significantly ( $p < 0.001$ ).

scirrhous gastric cancer cell lines (Figure 1). Subsequent *in vivo* studies revealed that intratumoral inoculation with G47Δ markedly inhibited tumor growth in subcutaneous tumor models (Figure 2). A low dose ( $2 \times 10^5$  PFU) inhibited tumor growth as effectively as with a high dose ( $1 \times 10^6$  PFU), presumably reflecting the good replication capability demonstrated in *in vitro* studies. In clinical settings, intratumoral G47Δ inoculation into gastric tumors using endoscopic devices is likely to become a principal means of treating the disease. We showed the efficacy and feasibility of intratumoral G47Δ inoculation in an orthotopic scirrhous gastric cancer model, which mimics the clinical situation of refractory gastric cancer (Figure 3).

Peritoneal dissemination is the most frequent pattern of recurrence or metastasis in gastric cancer patients, and also a major obstacle for improving the outcome.<sup>29</sup> Treatment approaches more effective than recently introduced anticancer drugs are required to treat peritoneal metastases.<sup>5</sup> Several oncolytic viruses and adenoviral vectors

have been used to investigate their efficacy in peritoneal dissemination models of gastric cancer,<sup>17–19,30,31</sup> whereas previous studies did not use a live bioluminescence imaging system, and none of them showed efficacy in a scirrhous gastric cancer model.<sup>19,31</sup> In the present study, intraperitoneal injections with G47Δ demonstrated high efficacy in two peritoneal dissemination models (Figure 4). Of note, G47Δ treatment remarkably prolonged the survival of mice bearing 44As3Luc peritoneal tumors that were rapidly fatal without G47Δ treatment owing to aggressive tumor progression. These findings together with the results from orthotopic models support the usefulness of G47Δ treatment for gastric cancer patients in advanced stages.

A selective replication of intraperitoneally injected G47Δ in metastatic tumors of the peritoneum was further confirmed in this study (Figure 5). An intratumoral inoculation is a reliable way to deliver G47Δ to target tumors;<sup>32</sup> however, in practice, it is difficult to inoculate tumor nodules scattered in the peritoneum with G47Δ without an

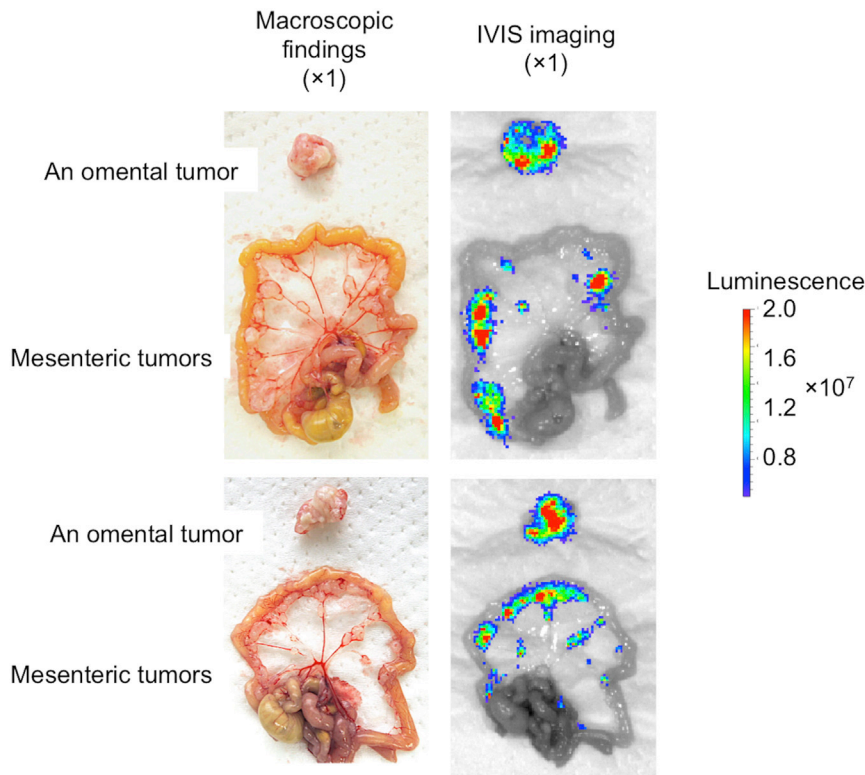


**Figure 5. The Distribution of Intraperitoneally Injected G47Δ in a Peritoneal Dissemination Model**

Peritoneal tumors were diffusely present in the omentum and mesentery. IVIS imaging revealed that T-luc, a luciferase-expressing oncolytic HSV-1 with the same backbone as G47Δ, was replicating selectively in metastatic tumors of the peritoneum ( $n = 2$ ).

invasive procedure. The present results suggest that G47Δ injected intraperitoneally can readily distribute to, and selectively replicate in, disseminated tumors without needing to inject the virus into each tumor nodule. Because ascites can contain a high concentration of antibodies, a possibility remains that intraperitoneally injected G47Δ can be attenuated in patients pre-exposed to HSV-1, as reported in a phase I study of oncolytic vaccinia virus for patients with peritoneal carcinomatosis.<sup>33</sup> Whereas no antibody can neutralize the activity of HSV-1 100%, the question awaits evaluation in future clinical trials.

Besides a direct cytotoxic activity, the potency of stimulating specific antitumor immunity is a crucial mechanism underlying the efficacy of oncolytic virus therapy.<sup>24,34</sup> Tumor cell deaths mediated by oncolytic viruses efficiently activate the interferon pathway and proinflammatory immune responses, causing subsequent accumulation of monocytes, active NK cells, and matured antigen-presenting cells, inducing a robust adaptive immune response.<sup>21</sup> G47Δ treatment elicits specific antitumor immunity that is further augmented by local expressions of immunostimulatory molecules such as soluble B7-1 and IL-12.<sup>22,23,25,28,35</sup> In addition, G47Δ treatment modifies immunosuppressive components of the tumor microenvironment such as regulatory T cells or immunosuppressive tumor-associated macrophages, resulting in facilitated trafficking of effector immune cells.<sup>25</sup>

Our study reveals that G47Δ treatment significantly increases the infiltration of inflammatory M1 macrophages and NK cells into the

tumor, while markedly decreasing the number of intratumoral immunosuppressive M2 macrophages, resulting in an increase in the M1-to-M2 ratio (Figures 6 and 7). Presumably, this macrophage polarization is initiated by the host immune response to viral infection, which swiftly recruits inflammatory macrophages and NK cells to the injected lesion.<sup>36</sup>

Such antiviral immune responses have been long considered to attenuate the efficacy of oncolytic HSV-1 by impeding its replication capability.<sup>36,37</sup> M1-polarized macrophages induced by oncolytic HSV-1 reportedly produce tumor necrosis factor (TNF)- $\alpha$ , which inhibits viral replication.<sup>38</sup> Similarly, NK cells have been suggested to restrict viral replication and spread.<sup>39</sup>

Alternatively, a recent study suggested that intratumoral macrophages induced by oncolytic virus treatment did not contribute to viral clearance.<sup>40</sup> Furthermore, emerging evidence has suggested that macrophage infiltration and M1-like polarization are necessary for a high efficacy of oncolytic virus therapy in immunocompetent mouse models,<sup>25,41</sup> and others have demonstrated that NK cells are important mediators of the antitumor effect associated with oncolytic virus therapy,<sup>42</sup> especially in the early phase.<sup>43</sup>

These findings support the notion that the innate immunity stimulated by oncolytic virus therapy may facilitate the priming of antitumor immunity; however, such a beneficial effect remains controversial and reportedly differs among the types of tumor and oncolytic virus.<sup>21,44</sup> Due to the lack of an appropriate immunocompetent mouse model for gastric cancer,<sup>45</sup> we could not evaluate the role of G47Δ-induced responses of macrophages and NK cells in adaptive antitumor immunity, which needs further investigation.

M2 macrophages have an immunosuppressive phenotype<sup>46</sup> and are generally associated with a poor outcome in patients with advanced gastric cancer and with peritoneal dissemination.<sup>47–49</sup> Also, a preclinical study highlighted the tumor-progressive feature of M2 macrophages using a subcutaneous gastric cancer model.<sup>49</sup> Whether the decrease of M2 macrophages in G47Δ-treated tumors is relevant to the improved efficacy needs further elucidation.

In summary, our results demonstrate that G47Δ is useful for treating human gastric cancer, including scirrhous gastric cancer and the ones

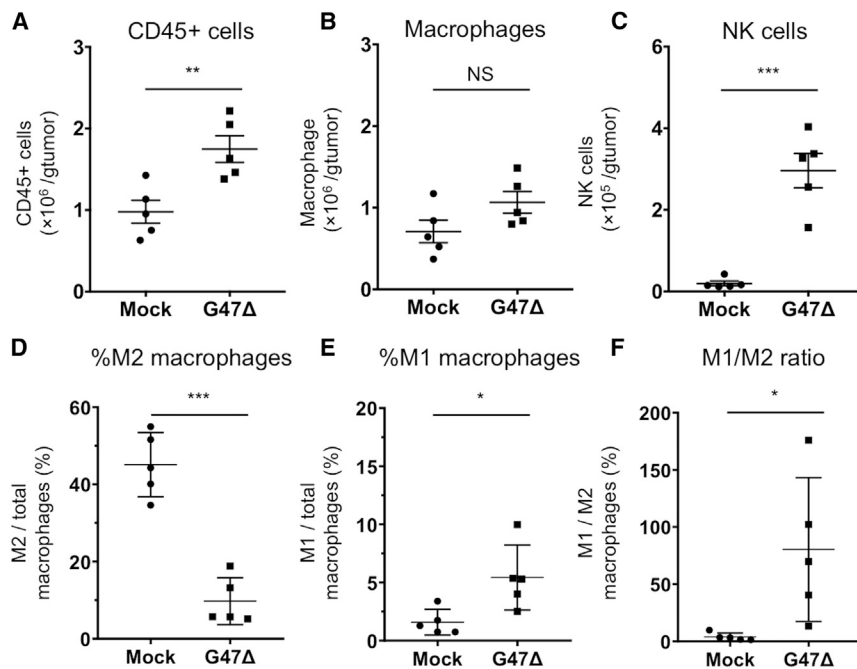


**Figure 6. Tumor-Infiltrating Lymphocytes in MKN45 Subcutaneous Tumors Treated with G47Δ**

Athymic mice bearing MKN45 subcutaneous tumors were inoculated intratumorally with G47Δ ( $1 \times 10^6$  PFU) or mock. Tumor tissues were harvested 2 days after these treatments. After removal of debris and doublets, tumor-infiltrating cells were stained with CD45-Brilliant Violet (BV) 785, CD11b-BV605, F4/80-APC, CD86-PE/Cy7, CD206-PE, and CD49b-FITC, followed by flow cytometric analysis. For all channels, positive and negative cells were gated on the basis of fluorescence minus one controls, and CD86 and CD206 were gated with appropriate isotype controls. (A–F) Absolute numbers of CD45<sup>+</sup> cells/g of tumor (A), absolute numbers of macrophages (CD45<sup>+</sup>CD11b<sup>+</sup>F4/80<sup>+</sup>)/g of tumor (B), absolute numbers of NK cells (CD45<sup>+</sup>CD49b<sup>+</sup>)/g of tumor (C), the ratio of M2 macrophages (CD206<sup>+</sup>CD86<sup>-</sup> macrophages) to total macrophages (D), the ratio of M1 macrophages (CD206<sup>-</sup>CD86<sup>+</sup> macrophages) to total macrophages (E), and the ratio of M1 macrophages to M2 macrophages (F) were compared between the two treatment groups. Bar represents mean  $\pm$  SEM ( $n = 5$ ). A Student's *t* test was used to determine the statistical significance (\* $p < 0.05$ , \*\* $p < 0.01$ , \*\*\* $p < 0.001$ ; NS, not significant).

in advanced stages. Further scrutiny is merited as to whether the innate immunity stimulated by G47Δ treatment can facilitate the antitumor effect of G47Δ.

## MATERIALS AND METHODS

### Cell Lines

Human gastric cancer cell lines MKN-1, MKN-45, MKN-74, NUGC-4, OCUM-1, and Kato III were obtained from the Japanese Collection of Research Bioresources (Osaka, Japan). Vero (African green monkey kidney) cells were purchased from the American Type Culture Collection (Rockville, MD, USA). Cells were cultured according to the directions provided by the suppliers. Human scirrhous gastric cancer cell lines 44As3, luciferase-expressing 44As3 (44As3Luc), HSC-60, and HSC-39 were established and cultured as previously described.<sup>20,50</sup> Luciferase-expressing MKN45 (MKN45-luc) cells were generated with pre-made luciferase lentiviral particles expressing the firefly luciferase3 gene (#LVP326, GenTarget) according to the manufacturer's protocol. Clonal selection was performed in a medium containing 10  $\mu$ g/mL blasticidin (Wako, Japan).

### Viruses

G47Δ was grown, purified, and titered by plaque assay on Vero cells as described previously.<sup>11,12</sup> T-luc<sup>CMV</sup> (T-luc), an oncolytic HSV-1 with the G47Δ backbone expressing the cytomegalovirus (CMV) promoter-regulated luciferase gene, was developed to demonstrate the viral distribution *in vivo* (unpublished data).

### Cytotoxicity Assays

*In vitro* cytotoxicity studies were performed as previously described.<sup>35</sup> Briefly, cells were seeded onto six-well plates at  $2 \times 10^5$  cells/well and

incubated overnight at 37°C. The following day, the cells were infected with G47Δ at various MOIs (0.01, 0.1, or 1) or mock, and further incubated in growth medium containing 1% heat-inactivated fetal calf serum (FCS) at 34.5°C. The number of surviving cells was counted daily with a Coulter Counter (Beckman Coulter, Fullerton, CA, USA) and expressed as a percentage of mock-infected controls. In the floating cells (OCUM-1, Kato III, and HSC-39), cell viability was determined with the CellTiter 96 Aqueous non-radioactive cell proliferation assay (Promega, Madison, WI, USA) according to the manufacturer's instructions. Briefly, the cells were seeded onto 96-well plates at the optimal cell density (OCUM-1,  $1 \times 10^4$  cells/well; Kato III,  $5 \times 10^3$  cells/well; HSC-39,  $9 \times 10^3$  cells/well) and were then infected with G47Δ (MOIs of 0.01, 0.1 or 1) or mock. The cell viability was determined daily and expressed as a percentage of mock-infected controls for each day.

### Virus Yield Studies

Cells were seeded onto six-well plates at  $3 \times 10^5$  cells/well and incubated overnight at 37°C. The following day, triplicate wells were infected with G47Δ at an MOI of 0.01. At 24 and 48 h after infection, the cells were scraped into the medium and lysed by three cycles of freezing and thawing. The progeny virus was titered as described previously.<sup>35</sup>

### Animal Experiments

All animal experiment protocols were approved by the Committee for Ethics of Animal Experimentation and were in accordance with the Guideline for Animal Experiments in the University of Tokyo. Six-week-old female athymic (BALB/c *nu/nu*) mice were purchased from CLEA Japan (Tokyo, Japan). The mice were maintained under

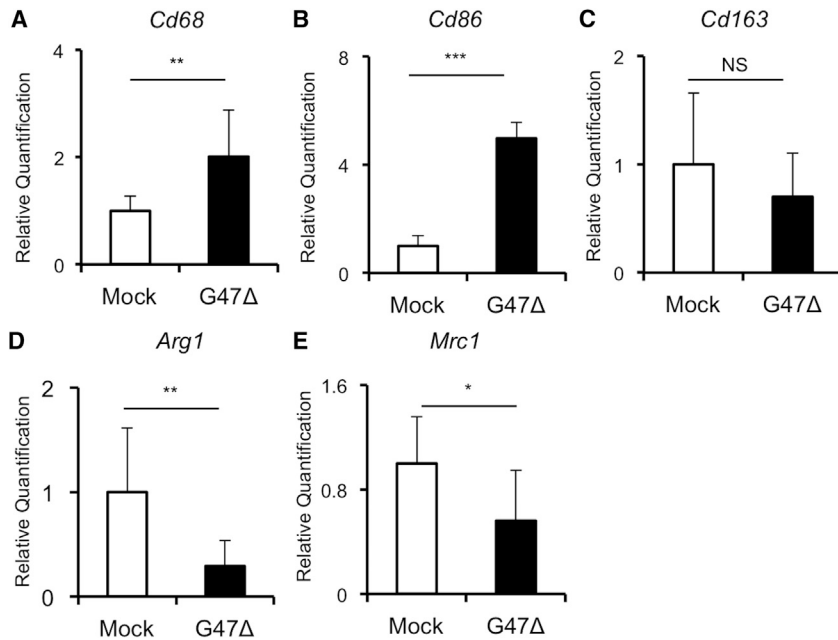


**Figure 7. Gene Expression Changes in MKN45 Subcutaneous Tumors Treated with G47Δ**

Athymic mice bearing MKN45 subcutaneous tumors were inoculated intratumorally with G47Δ ( $1 \times 10^6$  PFU) or mock. Tumor tissues were harvested 2 days after the treatments, total RNA was extracted, cDNA was reverse transcribed, and gene expression analysis was performed. (A–E) Gene expressions of (A) *Cd68*, (B) *Cd86*, (C) *Cd163*, (D) *Arg1*, and (E) *Mrc1* were compared between the two treatment groups. Expression data were normalized to the geometric mean of three housekeeping genes (*Actb*, *Gapdh*, and *Hprt1*). Bar represents mean relative quantification + SEM ( $n = 6$ ). A Student's *t* test was used to determine the statistical significance (\* $p < 0.05$ , \*\* $p < 0.01$ , \*\*\* $p < 0.001$ ; NS, not significant).

specific pathogen-free conditions and provided with sterile food, water, and cages.

#### Subcutaneous Tumor Models

Subcutaneous tumors of gastric cancer were generated by inoculating  $1 \times 10^6$  cells (MKN74, 44As3) or  $5 \times 10^6$  cells (MKN45) into the left flanks of 6-week-old female athymic mice (BALB/*nu/nu*). When tumors reached approximately 5–7 mm in diameter, the animals were randomized, and mock or G47Δ ( $2 \times 10^5$  or  $1 \times 10^6$  PFU) in 20  $\mu$ L of phosphate-buffered saline (PBS) containing 10% glycerol was inoculated into the left-flank tumors. Mock-infected extract was prepared from virus buffer-infected cells employing the same procedures as those used for the virus inoculum.<sup>22</sup> Intratumoral G47Δ injection was repeated 3 days later. For evaluating the efficacy of G47Δ for large tumors, athymic mice harboring MKN45 and 44As3 tumors were inoculated intratumorally with G47Δ ( $1 \times 10^6$  PFU) or mock three times (days 0, 2, and 4) when the tumor volumes exceeded 200 mm<sup>3</sup>. The tumor volume (length  $\times$  width  $\times$  height) was measured twice a week. Mice were sacrificed when the maximum diameter of the tumor reached 24 mm.

For *in vivo* flow cytometry experiments, mice with established MKN45 subcutaneous tumors were given a single intratumoral inoculation with mock or G47Δ ( $1 \times 10^6$  PFU). Two days later, subcutaneous tumors were harvested, stained for immune markers, and analyzed by flow cytometry (see below).

#### An Orthotopic Tumor Model of Scirrhous Gastric Cancer

Orthotopic implantation of 44As3Luc cells ( $1 \times 10^6$  cells) was performed in 6-week-old female athymic mice as previously described.<sup>20</sup>

Briefly, a small median abdominal incision was made under anesthesia. 44As3Luc cells ( $2 \times 10^6$  cells) in a 20- $\mu$ L volume of RPMI 1640 medium were inoculated into the middle wall of the greater curvature of the stomach with a 30G needle (Nipro, Tokyo, Japan). The stomach was then returned to the peritoneal cavity, and the abdominal wall and skin were closed with 5-0 PDS suture. Seven days after tumor cell inoculation (on day 7), orthotopic tumor volume was determined by bioluminescence imaging with an IVIS (IVIS Lumina Series III, SPI, Japan) and the mice were divided into two groups. On days 8 and 11, the mice were inoculated intratumorally with mock or G47Δ ( $2 \times 10^6$  PFU) in 20  $\mu$ L of PBS containing 10% glycerol. The total photon counts of orthotopic tumors and survival were observed. *In vivo* photon counting analysis was conducted twice a week on the IVIS with Living Image 4.4. acquisition and analysis software (Xenogen, USA) as previously described.<sup>51</sup>

#### Peritoneal Dissemination Models

Peritoneal dissemination models of gastric cancer were established by intraperitoneal injection of MKN45-luc cells ( $5 \times 10^6$  cells) or 44As3Luc cells ( $1 \times 10^6$  cells) into 6-week-old female athymic mice. Three days after tumor cell injection (on day 3), peritoneal tumor volume was determined by bioluminescence imaging with IVIS and the mice were divided into two groups according to tumor volumes. On days 4 and 7, the mice were injected intraperitoneally with mock or G47Δ ( $1 \times 10^6$  PFU) in 100  $\mu$ L of PBS. Total photon counts of peritoneal tumors and survival were observed.

Intraperitoneal distributions of G47Δ were studied by T-luc injection into the abdominal cavities of athymic mice with MKN45 peritoneal tumors. MKN45 cells ( $5 \times 10^6$  cells) were injected into the peritoneal cavities of 6-week-old female athymic mice. Seventeen days later (on day 17), T-luc ( $2 \times 10^6$  PFU) in 100  $\mu$ L of PBS was injected intraperitoneally. Four days later (on day 21), the mice were sacrificed and the intraperitoneal virus distribution was studied with bioluminescence imaging.



### Flow Cytometry

Tumor-infiltrating cells were prepared with a tumor dissociation kit (Miltenyi Biotec, Auburn, CA, USA) according to the manufacturer's instructions. The total number of live cells analyzed was matched between the groups with Flow Count beads (Beckman Coulter, Fullerton, CA, USA). A Zombie Yellow fixable viability kit (BioLegend, San Diego, CA, USA) was used to stain dead cells. The cells were then pretreated with purified anti-mouse CD16/32 (2.4G2) (BD Biosciences, NJ, USA), stained with antibodies, and analyzed with a CytoFLEX (V5-B5-R3 configuration, Beckman Coulter, Fullerton, CA, USA). The following fluorescent-labeled antibodies were purchased from BioLegend (San Diego, CA, USA) and used for analysis: Brilliant Violet 785-conjugated anti-CD45 (30-F11), Brilliant Violet 605-conjugated anti CD11b (M1/70), allophycocyanin (APC)-conjugated anti-F4/80 (BM8), phycoerythrin (PE)-Cyanine7-conjugated anti-CD86 (GL-1), PE-conjugated anti-CD206 (MMR), and fluorescein isothiocyanate (FITC)-conjugated anti-CD49b (HM $\alpha$ 2). For all channels, positive and negative cells were gated on the basis of fluorescence minus one controls, and CD86 and CD206 were gated with appropriate isotype controls (Figure S1). The data were analyzed with FlowJo software v10.4.

### Extraction of RNA and Real-Time Quantitative PCR

Athymic mice bearing MKN45 subcutaneous tumors were treated with a single intratumoral inoculation with mock or G47 $\Delta$  ( $1 \times 10^6$  PFU). Two days later, the tumors were excised and snap-frozen in liquid nitrogen. The samples were homogenized, and RNA was extracted using the RNeasy mini kit (QIAGEN) and QIAcube according to the manufacturer's instructions. RNA purity and yield were assessed using NanoDrop. RNA was reverse transcribed to cDNA using the ReverTra Ace qPCR RT master mix with genomic DNA (gDNA) remover (Toyobo). The samples were stored at  $-20^{\circ}\text{C}$  until real-time PCR was performed. Real-time quantitative PCR on 15 ng of cDNA from each sample ( $n = 6$ ) was performed using TaqMan gene expression assays (Thermo Fisher Scientific) and the QuantStudio 7 Flex real-time PCR system (Thermo Fisher Scientific). Expression data for individual samples were normalized to the geometric mean of three housekeeping genes (HKGs): *Actb*, *Gapdh*, and *Hprt1*. The fold change in gene expression (relative quantification) was calculated using Expression Suite software version 1.0.3 (Life Technologies), a data analysis tool that utilizes the comparative Ct ( $\Delta\Delta\text{Ct}$ ) method.

### Statistical Analysis

All data were expressed as the mean  $\pm$  standard deviation (SD) or the mean  $\pm$  standard error of the mean (SEM). A two-tailed Student's *t* test or the Mann-Whitney nonparametric test (for comparison of two groups) or one-way ANOVA followed by Dunnett's test (for comparison of three or more groups) was used to determine statistical significance, as appropriate. The survival curves were analyzed by the Kaplan-Meier method, and  $p < 0.05$  was considered as statistically significant using the log rank test. In the figures, standard symbols are used as follows: \* $p < 0.05$ , \*\* $p < 0.01$ , \*\*\* $p < 0.001$ ; NS, not significant. Statistical analyses were carried out with JMP 13.0.0 (SAS Institute, Cary, NC, USA).

### SUPPLEMENTAL INFORMATION

Supplemental Information can be found online at <https://doi.org/10.1016/j.omto.2020.03.022>.

### AUTHOR CONTRIBUTIONS

K.S. and T.T. were involved with the conception and performance of experiments, statistical analysis, interpretation of results, and writing the manuscript. M.I. assisted with some of the experiments. S.Y. and M.T. were involved with the conception and design of experiments. K.Y. offered cell lines. Y.S. participated in manuscript preparation. All authors reviewed and edited the manuscript.

### CONFLICTS OF INTEREST

T.T. owns the patent right for G47 $\Delta$  in Japan.

### ACKNOWLEDGMENTS

This research was supported in part by grants to T.T. from Practical Research for Innovative Cancer Control, Japan Agency for Medical Research and Development (AMED) (grant JP19ck0106416), and by the Translational Research Program, AMED (grant JP19lm0203004).

### REFERENCES

1. Siegel, R.L., Miller, K.D., and Jemal, A. (2015). Cancer statistics, 2015. *CA Cancer J. Clin.* 65, 5–29.
2. Ajani, J.A., Lee, J., Sano, T., Janjigian, Y.Y., Fan, D., and Song, S. (2017). Gastric adenocarcinoma. *Nat. Rev. Dis. Primers* 3, 17036.
3. Wilke, H., Muro, K., Van Cutsem, E., Oh, S.C., Bodoky, G., Shimada, Y., Hironaka, S., Sugimoto, N., Lipatov, O., Kim, T.Y., et al.; RAINBOW Study Group (2014). Ramucirumab plus paclitaxel versus placebo plus paclitaxel in patients with previously treated advanced gastric or gastro-oesophageal junction adenocarcinoma (RAINBOW): a double-blind, randomised phase 3 trial. *Lancet Oncol.* 15, 1224–1235.
4. Kang, Y.K., Boku, N., Satoh, T., Ryu, M.H., Chao, Y., Kato, K., Chung, H.C., Chen, J.S., Muro, K., Kang, W.K., et al. (2017). Nivolumab in patients with advanced gastric or gastro-oesophageal junction cancer refractory to, or intolerant of, at least two previous chemotherapy regimens (ONO-4538-12, ATTRACTION-2): a randomised, double-blind, placebo-controlled, phase 3 trial. *Lancet* 390, 2461–2471.
5. Ishigami, H., Fujiwara, Y., Fukushima, R., Nashimoto, A., Yabusaki, H., Imano, M., Imamoto, H., Kodera, Y., Uenosono, Y., Amagai, K., et al. (2018). Phase III trial comparing intraperitoneal and intravenous paclitaxel plus S-1 versus cisplatin plus S-1 in patients with gastric cancer with peritoneal metastasis: PHOENIX-GC trial. *J. Clin. Oncol.* 36, 1922–1929.
6. Yamaguchi, H., and Sakai, R. (2015). Direct interaction between carcinoma cells and cancer associated fibroblasts for the regulation of cancer invasion. *Cancers (Basel)* 7, 2054–2062.
7. Nakamura, R., Saikawa, Y., Wada, N., Yoshida, M., Kubota, T., Kumai, K., and Kitajima, M. (2007). Retrospective analysis of prognosis for scirrhous-type gastric cancer: one institution's experience. *Int. J. Clin. Oncol.* 12, 291–294.
8. Fukuhara, H., Ino, Y., and Todo, T. (2016). Oncolytic virus therapy: a new era of cancer treatment at dawn. *Cancer Sci.* 107, 1373–1379.
9. Yokoda, R., Nagalo, B.M., Arora, M., Egan, J.B., Bogenberger, J.M., DeLeon, T.T., Zhou, Y., Ahn, D.H., and Borad, M.J. (2018). Oncolytic virotherapy in upper gastrointestinal tract cancers. *Oncolytic Virother.* 7, 13–24.
10. Andtbacka, R.H., Kaufman, H.L., Collichio, F., Amatruda, T., Senzer, N., Chesney, J., Delman, K.A., Spitzer, L.E., Puzanov, I., Agarwala, S.S., et al. (2015). Talimogene laherparepvec improves durable response rate in patients with advanced melanoma. *J. Clin. Oncol.* 33, 2780–2788.

11. Todo, T., Martuza, R.L., Rabkin, S.D., and Johnson, P.A. (2001). Oncolytic herpes simplex virus vector with enhanced MHC class I presentation and tumor cell killing. *Proc. Natl. Acad. Sci. USA* 98, 6396–6401.
12. Mineta, T., Rabkin, S.D., Yazaki, T., Hunter, W.D., and Martuza, R.L. (1995). Attenuated multi-mutated herpes simplex virus-1 for the treatment of malignant gliomas. *Nat. Med.* 1, 938–943.
13. Fukuhara, H., Martuza, R.L., Rabkin, S.D., Ito, Y., and Todo, T. (2005). Oncolytic herpes simplex virus vector G47 $\Delta$  in combination with androgen ablation for the treatment of human prostate adenocarcinoma. *Clin. Cancer Res.* 11, 7886–7890.
14. Fukuhara, H., Ino, Y., Kuroda, T., Martuza, R.L., and Todo, T. (2005). Triple gene-deleted oncolytic herpes simplex virus vector double-armed with interleukin 18 and soluble B7-1 constructed by bacterial artificial chromosome-mediated system. *Cancer Res.* 65, 10663–10668.
15. Tsuji, T., Nakamori, M., Iwahashi, M., Nakamura, M., Ojima, T., Iida, T., Katsuda, M., Hayata, K., Ino, Y., Todo, T., and Yamaue, H. (2013). An armed oncolytic herpes simplex virus expressing thrombospondin-1 has an enhanced in vivo antitumor effect against human gastric cancer. *Int. J. Cancer* 132, 485–494.
16. Sui, H., Wang, K., Xie, R., Li, X., Li, K., Bai, Y., Wang, X., Bai, B., Chen, D., Li, J., and Shen, B. (2017). NDV-D90 suppresses growth of gastric cancer and cancer-related vascularization. *Oncotarget* 8, 34516–34524.
17. Kawaguchi, K., Etoh, T., Suzuki, K., Mitui, M.T., Nishizono, A., Shiraishi, N., and Kitano, S. (2010). Efficacy of oncolytic reovirus against human gastric cancer with peritoneal metastasis in experimental animal model. *Int. J. Oncol.* 37, 1433–1438.
18. Zhou, W., Dai, S., Zhu, H., Song, Z., Cai, Y., Lee, J.B., Li, Z., Hu, X., Fang, B., He, C., and Huang, X. (2017). Telomerase-specific oncolytic adenovirus expressing TRAIL suppresses peritoneal dissemination of gastric cancer. *Gene Ther.* 24, 199–207.
19. Natatsuka, R., Takahashi, T., Serada, S., Fujimoto, M., Ookawara, T., Nishida, T., Hara, H., Nishigaki, T., Harada, E., Murakami, T., et al. (2015). Gene therapy with SOCS1 for gastric cancer induces G2/M arrest and has an antitumor effect on peritoneal carcinomatosis. *Br. J. Cancer* 113, 433–442.
20. Yanagihara, K., Takigahira, M., Takeshita, F., Komatsu, T., Nishio, K., Hasegawa, F., and Ochiya, T. (2006). A photon counting technique for quantitatively evaluating progression of peritoneal tumor dissemination. *Cancer Res.* 66, 7532–7539.
21. Gujar, S., Pol, J.G., Kim, Y., Lee, P.W., and Kroemer, G. (2018). Antitumor benefits of antiviral immunity: an underappreciated aspect of oncolytic virotherapies. *Trends Immunol.* 39, 209–221.
22. Todo, T., Martuza, R.L., Dallman, M.J., and Rabkin, S.D. (2001). In situ expression of soluble B7-1 in the context of oncolytic herpes simplex virus induces potent antitumor immunity. *Cancer Res.* 61, 153–161.
23. Nakatake, R., Kaibori, M., Nakamura, Y., Tanaka, Y., Matushima, H., Okumura, T., Murakami, T., Ino, Y., Todo, T., and Kon, M. (2018). Third-generation oncolytic herpes simplex virus inhibits the growth of liver tumors in mice. *Cancer Sci.* 109, 600–610.
24. Kaufman, H.L., Kohlhapp, F.J., and Zloza, A. (2015). Oncolytic viruses: a new class of immunotherapy drugs. *Nat. Rev. Drug Discov.* 14, 642–662.
25. Saha, D., Martuza, R.L., and Rabkin, S.D. (2017). Macrophage polarization contributes to glioblastoma eradication by combination immunovirotherapy and immune checkpoint blockade. *Cancer Cell* 32, 253–267.e5.
26. Cheema, T.A., Kanai, R., Kim, G.W., Wakimoto, H., Passer, B., Rabkin, S.D., and Martuza, R.L. (2011). Enhanced antitumor efficacy of low-dose etoposide with oncolytic herpes simplex virus in human glioblastoma stem cell xenografts. *Clin. Cancer Res.* 17, 7383–7393.
27. Aghi, M., Rabkin, S.D., and Martuza, R.L. (2007). Angiogenic response caused by oncolytic herpes simplex virus-induced reduced thrombospondin expression can be prevented by specific viral mutations or by administering a thrombospondin-derived peptide. *Cancer Res.* 67, 440–444.
28. Ino, Y., Saeki, Y., Fukuhara, H., and Todo, T. (2006). Triple combination of oncolytic herpes simplex virus-1 vectors armed with interleukin-12, interleukin-18, or soluble B7-1 results in enhanced antitumor efficacy. *Clin. Cancer Res.* 12, 643–652.
29. Kobayashi, D., and Kodera, Y. (2017). Intraperitoneal chemotherapy for gastric cancer with peritoneal metastasis. *Gastric Cancer* 20 (Suppl 1), 111–121.
30. Bennett, J.J., Delman, K.A., Burt, B.M., Mariotti, A., Malhotra, S., Zager, J., Petrowsky, H., Mastorides, S., Federoff, H., and Fong, Y. (2002). Comparison of safety, delivery, and efficacy of two oncolytic herpes viruses (G207 and NV1020) for peritoneal cancer. *Cancer Gene Ther.* 9, 935–945.
31. Haley, E.S., Au, G.G., Carlton, B.R., Barry, R.D., and Shafren, D.R. (2009). Regional administration of oncolytic echovirus 1 as a novel therapy for the peritoneal dissemination of gastric cancer. *J. Mol. Med. (Berl.)* 87, 385–399.
32. Chahnavi, A., Rabkin, S., Todo, T., Sundaresan, P., and Martuza, R. (1999). Effect of prior exposure to herpes simplex virus 1 on viral vector-mediated tumor therapy in immunocompetent mice. *Gene Ther.* 6, 1751–1758.
33. Lauer, U.M., Schell, M., Beil, J., Berchtold, S., Koppenhöfer, U., Glatzle, J., Königsrainer, A., Möhle, R., Nann, D., Fend, F., et al. (2018). Phase I study of oncolytic vaccinia virus GL-ONC1 in patients with peritoneal carcinomatosis. *Clin. Cancer Res.* 24, 4388–4398.
34. Kaufman, H.L., Kim, D.W., DeRaffele, G., Mitcham, J., Coffin, R.S., and Kim-Schulze, S. (2010). Local and distant immunity induced by intralesional vaccination with an oncolytic herpes virus encoding GM-CSF in patients with stage IIIc and IV melanoma. *Ann. Surg. Oncol.* 17, 718–730.
35. Todo, T., Rabkin, S.D., Sundaresan, P., Wu, A., Meehan, K.R., Herscovitz, H.B., and Martuza, R.L. (1999). Systemic antitumor immunity in experimental brain tumor therapy using a multimitated, replication-competent herpes simplex virus. *Hum. Gene Ther.* 10, 2741–2755.
36. Alvarez-Breckenridge, C.A., Yu, J., Price, R., Wojton, J., Pradarelli, J., Mao, H., Wei, M., Wang, Y., He, S., Hardcastle, J., et al. (2012). NK cells impede glioblastoma virotherapy through NKp30 and NKp46 natural cytotoxicity receptors. *Nat. Med.* 18, 1827–1834.
37. Fulci, G., Dmitrieva, N., Gianni, D., Fontana, E.J., Pan, X., Lu, Y., Kaufman, C.S., Kaur, B., Lawler, S.E., Lee, R.J., et al. (2007). Depletion of peripheral macrophages and brain microglia increases brain tumor titers of oncolytic viruses. *Cancer Res.* 67, 9398–9406.
38. Meisen, W.H., Wohleb, E.S., Jaime-Ramirez, A.C., Bolyard, C., Yoo, J.Y., Russell, L., Hardcastle, J., Dubin, S., Muili, K., Yu, J., et al. (2015). The impact of macrophage- and microglia-secreted TNF $\alpha$  on oncolytic HSV-1 therapy in the glioblastoma tumor microenvironment. *Clin. Cancer Res.* 21, 3274–3285.
39. Fulci, G., Breyman, L., Gianni, D., Kurozumi, K., Rhee, S.S., Yu, J., Kaur, B., Louis, D.N., Weissleder, R., Caligiuri, M.A., and Chiocca, E.A. (2006). Cyclophosphamide enhances glioma virotherapy by inhibiting innate immune responses. *Proc. Natl. Acad. Sci. USA* 103, 12873–12878.
40. Zemp, F.J., McKenzie, B.A., Lun, X., Reilly, K.M., McFadden, G., Yong, V.W., and Forsyth, P.A. (2014). Cellular factors promoting resistance to effective treatment of glioma with oncolytic myxoma virus. *Cancer Res.* 74, 7260–7273.
41. Kleijn, A., Kloezeman, J., Treffers-Westerlaken, E., Fulci, G., Leenstra, S., Dirven, C., Debets, R., and Lamfers, M. (2014). The in vivo therapeutic efficacy of the oncolytic adenovirus Delta24-RGD is mediated by tumor-specific immunity. *PLoS ONE* 9, e97495.
42. Zamarin, D., Holmgaard, R.B., Subudhi, S.K., Park, J.S., Mansour, M., Palese, P., Merghoub, T., Wolchok, J.D., and Allison, J.P. (2014). Localized oncolytic virotherapy overcomes systemic tumor resistance to immune checkpoint blockade immunotherapy. *Sci. Transl. Med.* 6, 226ra32.
43. Zamarin, D., Ricca, J.M., Sadekova, S., Oseledchik, A., Yu, Y., Blumenschein, W.M., Wong, J., Gigoux, M., Merghoub, T., and Wolchok, J.D. (2018). PD-L1 in tumor microenvironment mediates resistance to oncolytic immunotherapy. *J. Clin. Invest.* 128, 1413–1428.
44. Denton, N.L., Chen, C.Y., Scott, T.R., and Cripe, T.P. (2016). Tumor-associated macrophages in oncolytic virotherapy: friend or foe? *Biomedicines* 4, E13.
45. Yamamoto, M., Nomura, S., Hosoi, A., Nagaoka, K., Iino, T., Yasuda, T., Saito, T., Matsushita, H., Uchida, E., Seto, Y., et al. (2018). Established gastric cancer cell lines transplantable into C57BL/6 mice show fibroblast growth factor receptor 4 promotion of tumor growth. *Cancer Sci* 109, 1480–1492.
46. Biswas, S.K., and Mantovani, A. (2010). Macrophage plasticity and interaction with lymphocyte subsets: cancer as a paradigm. *Nat. Immunol.* 11, 889–896.

47. Rojas, A., Delgado-López, F., and Gonzalez, I. (2017). Tumor-associated macrophages in gastric cancer: more than bystanders in tumor microenvironment. *Gastric Cancer* 20, 215–216.
48. Zhang, H., Wang, X., Shen, Z., Xu, J., Qin, J., and Sun, Y. (2015). Infiltration of diametrically polarized macrophages predicts overall survival of patients with gastric cancer after surgical resection. *Gastric Cancer* 18, 740–750.
49. Yamaguchi, T., Fushida, S., Yamamoto, Y., Tsukada, T., Kinoshita, J., Oyama, K., Miyashita, T., Tajima, H., Ninomiya, I., Munesue, S., et al. (2016). Tumor-associated macrophages of the M2 phenotype contribute to progression in gastric cancer with peritoneal dissemination. *Gastric Cancer* 19, 1052–1065.
50. Fujita, T., Yanagihara, K., Takeshita, F., Aoyagi, K., Nishimura, T., Takigahira, M., Chiwaki, F., Fukagawa, T., Katai, H., Ochiya, T., et al. (2013). Intraperitoneal delivery of a small interfering RNA targeting *NEDD1* prolongs the survival of scirrhous gastric cancer model mice. *Cancer Sci.* 104, 214–222.
51. Toyoshima, M., Tanaka, Y., Matumoto, M., Yamazaki, M., Nagase, S., Sugamura, K., and Yaegashi, N. (2009). Generation of a syngeneic mouse model to study the intraperitoneal dissemination of ovarian cancer with in vivo luciferase imaging. *Luminescence* 24, 324–331.

OMTO, Volume 17

## **Supplemental Information**

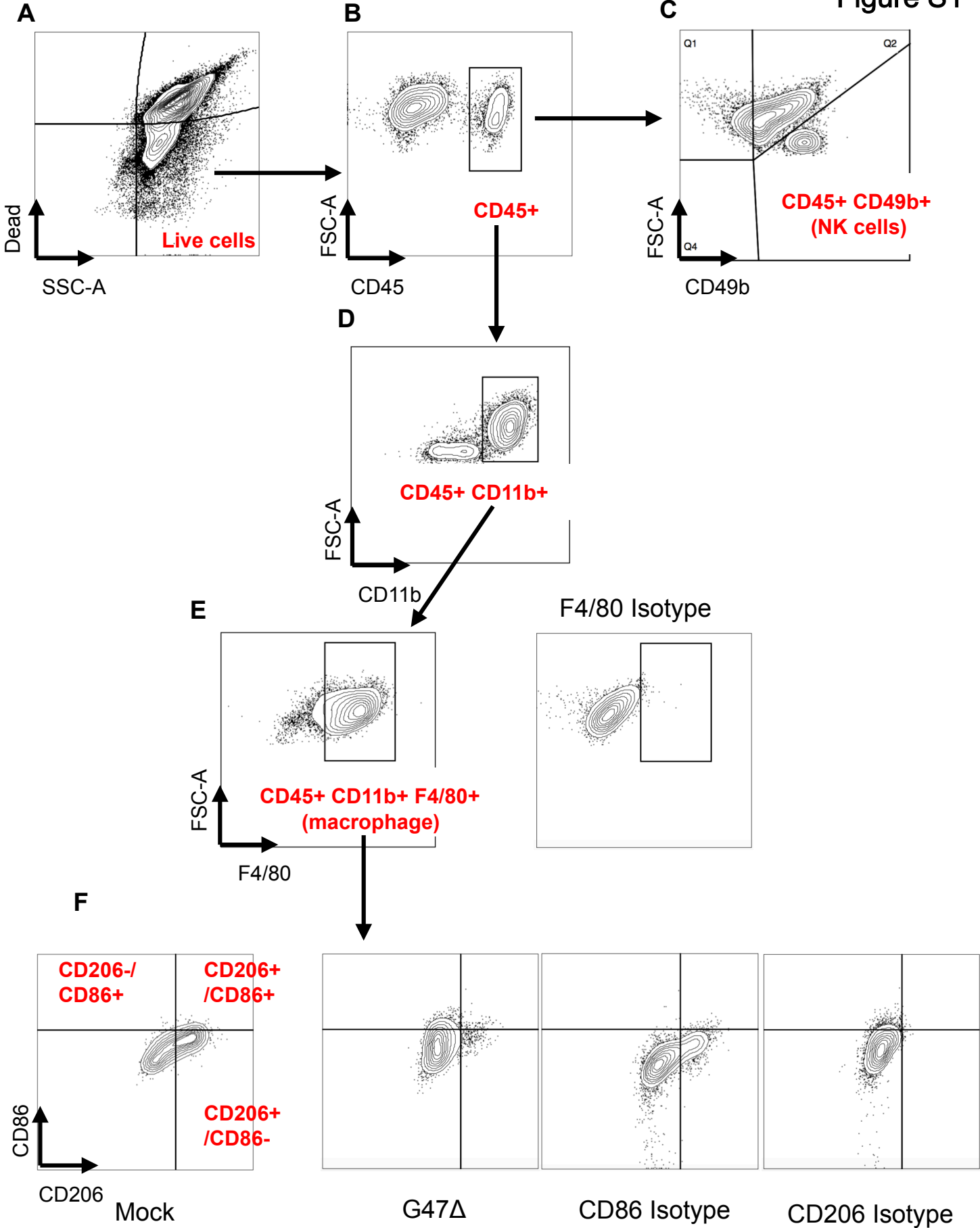
**Efficacy of a Third-Generation Oncolytic**

**Herpes Virus G47 $\Delta$  in Advanced Stage**

**Models of Human Gastric Cancer**

**Kotaro Sugawara, Miwako Iwai, Shoh Yajima, Minoru Tanaka, Kazuyoshi  
Yanagihara, Yasuyuki Seto, and Tomoki Todo**

Figure S1



## **Supplemental Figure 1. Gating strategy**

Representative flow cytometry plots and the gating strategy are shown. (A, B, D, E) Macrophages were assessed as CD45<sup>+</sup>CD11b<sup>+</sup> F4/80<sup>+</sup> after dead cells and doublets were removed. (C) NK cells were defined as CD45<sup>+</sup>CD49b<sup>+</sup>. (F) M1 macrophages (CD86<sup>+</sup>CD206<sup>-</sup> macrophages) and M2 macrophages (CD86<sup>-</sup>CD206<sup>+</sup> macrophages) were determined based on the each isotype control.